Neurological Sciences (2020) 41:347–355
https://doi.org/10.1007/s10072-019-04087-9

ORIGINAL ARTICLE

In vivo 2-hydroxyglutarate-proton magnetic resonance spectroscopy (3 T, PRESS technique) in treatment-naïve suspect lower-grade gliomas: feasibility and accuracy in a clinical setting

Valeria Cuccarini[1] · Luigi Antelmi[1] · Bianca Pollo[2] · Rosina Paterra[3] · Chiara Calatozzolo[2] · Anna Nigri[1] · Francesco DiMeco[4] · Marica Eoli[3] · Gaetano Finocchiaro[3] · Greta Brenna[5] · Irene Tramacere[5] · Maria Grazia Bruzzone[1] · Elena Anghileri[3]

Received: 24 March 2019 / Accepted: 24 September 2019 / Published online: 24 October 2019

Abstract

Isocitrate dehydrogenase 1/2 (*IDH1/2*) mutations are often detected in lower-grade gliomas (LGG) and result into 2-hydroxyglutarate (2HG) synthesis. Prior studies showed that 2HG can be detected in vivo using magnetic resonance spectroscopy (MRS), but its accuracy and translational impact are still under investigation.

Purpose To investigate the clinical feasibility of MRS for in vivo detection and quantification of 2HG on consecutive treatment-naïve suspect LGG patients and to compare MRS accuracy with tissue IDH1/2 analysis.

Methods MRS spectra at 3 T were acquired with 1H-MRS single-voxel PRESS 2HG-tailored sequences with TE 30 (group 1) or TE 97 (groups 2A and B). Voxel sizes were 1.5 × 1.5 × 1.5 cm^3 for group 1 ($n = 13$) and group 2A ($n = 14$) and 2 × 2 × 2 cm^3 for group 2B ($n = 32$). Multiple metabolites' concentrations were analyzed with LCModel. Tumors were assessed for IDH status and main molecular markers. 2HG levels in urine/blood were measured by liquid chromatography–mass spectrometry.

Results The larger voxel TE 97 sequence resulted in highest specificity (100%), sensitivity (79%), and accuracy (87%). Urine and blood 2HG did not result predictive.

Conclusion Our data confirm that 2 × 2 × 2-cm^3 voxel TE 97 MRS shows high accuracy for 2HG detection, with good sensitivity and 100% specificity in distinguishing IDH mutant gliomas. Main limits of the technique are small tumor volume and low cellularity. Integrating 2HG-MRS with other metabolites may help non-invasive diagnosis of glioma, prognostic assessment, and treatment planning in clinical setting.

Keywords Glioma · 2-hydroxyglutarate (2HG) · Magnetic resonance spectroscopy (MRS) · Isocitrate dehydrogenase (IDH) · Point-resolved spectroscopy (PRESS)

Introduction

Recently the classification of lower-grade gliomas (LGG) has included the isocitrate dehydrogenase 1/2 (*IDH1/2*) mutations and 1p19q codeletion as major main molecular parameters [1].

IDH1/2 converts isocitrate to α-ketoglutarate respectively in the cytosol and in mitochondria, and its mutations result in

Electronic supplementary material The online version of this article (https://doi.org/10.1007/s10072-019-04087-9) contains supplementary material, which is available to authorized users.

✉ Elena Anghileri
elena.anghileri@istituto-besta.it

[1] Unit of Neuroradiology, Fondazione Irccs Istituto Neurologico Carlo Besta, Via Celoria 11, Milan, Italy

[2] Neuropathology, Fondazione Irccs Istituto Neurologico Carlo Besta, Milan, Italy

[3] Unit of Molecular Neuro-Oncology, Fondazione Irccs Istituto Neurologico Carlo Besta, Milan, Italy

[4] Department Neurosurgery Department, Fondazione Irccs Istituto Neurologico Carlo Besta, Milan Italy

[5] Department of Research and Clinical Development, Scientific Directorate, Fondazione Irccs Istituto Neurologico Carlo Besta, Milan, Italy

the accumulation of 2-hydroxyglutarate (2HG), with intracellular concentrations on the order of millimolar [2]. Mutations in the *IDH* genes are reported in up to 70–80% of LGG and secondary glioblastomas (GBM), while in less than 10% of primary GBM.

The most frequent (up to 93%) is *IDH1* mutation R132H (c.395G > A), detectable by immunohistochemistry (IHC) on tissue samples, while the remaining *IDH1/2* mutations require direct sequencing [3].

IDH mutant (*IDH*mut) gliomas show distinct characteristics relative to *IDH* wild type (wt) and are associated to better prognosis, and identifying *IDH* mutations is important to tailor therapeutic approach [4]. Magnetic resonance imaging (MRI) is an ideal candidate for non-invasively providing in vivo biomarkers, including 2HG detection by MR spectroscopy (MRS) to predict *IDH* status [5, 6]. Detection of 2HG on biological fluids has been also proposed, but this approach is not yet confirmed in glioma [7].

The intracerebral accumulation of 2HG cannot be detected by standard MRS because of the structural complexity of the molecule that gives rise to multiplets resonating at three frequencies at 3 T (1.9, 2.25, and 4.02 ppm) whose spectrum overlaps those, greater, of N-acetyl-aspartate (NAA) and glutamate (Glu) [8, 9]. Specific MRS sequences have been implemented since 2012 to identify and quantify in vivo 2HG in patients affected by *IDH*mut gliomas, based on 2HG accumulation in *IDH*mut tumors [10–12].

Different MRS techniques have been used to determine 2HG in vivo in glioma patients (Table 1) reporting a range of accuracy depending on multiple factors including technical characteristics as the field strength, technique, and echo times and on tumoral features as location, volume, and cellularity [5, 9–29].

The aim of the present study was to determine the clinical feasibility and accuracy of different 2HG-tailored MRS PRESS sequences at 3 T in treatment-naïve, suspected LGG. As secondary aims, we investigated the associations with tumor location, histopathology, main molecular features, and concentrations of other metabolites. Preliminary analyses of 2HG level on plasma and urine were also performed.

Patients and methods

Patients

This prospective, observational study of in vivo MRS detection and quantification of 2HG in treatment-naïve suspected LGG was performed at the Fondazione IRCCS Istituto Neurologico Carlo Besta, Milan, Italy. The Institutional Ethics Committee approved the study (protocol n. 419/2014), which conforms to the Declaration of Helsinki. Informed consent was obtained from all participants.

Between 2014 and 2016, all consecutive adult patients with suspected brain LGG according to pre-surgical conventional MRI (cMRI) were considered for inclusion.

A glioma was suspected to be lower-grade when no necrosis or relevant edema (i.e., absence of edema or minimal edema not distinguishable from tumor burden) was observed and when contrast enhancement was absent or faint on cMRI.

Patients who had already undergone biopsy/surgery or treated with chemo- or radiotherapy were excluded.

Enrolled patients underwent MRS during the pre-surgical MRI.

Magnetic resonance imaging

MRI was performed on a Philips Achieva 3 T scanner with a 32 channel head coil.

Whole brain multiplanar T1- and T2-weighted images, fluid-attenuated inversion recovery (FLAIR), and diffusion-weighted imaging (DWI, b = 0 and 1000 s/mm^2) were acquired and used for guidance in the positioning of the spectroscopic voxel.

Contrast-enhanced T13D sequence was acquired after MRS.

On DWI, the apparent diffusion coefficient (ADC) value was calculated within a region of interest (ROI) corresponding to the MRS voxel site. A senior neuroradiologist placed circular ROIs in different areas of the lesion and one in the CHWM. The ROIs were placed on the basis of cMRI and ADC map appearance in order to select the areas of supposed highest cell density (inversely proportional to ADC). The tumoral ADC values were normalized (rADC) to those obtained from the CHWM. The MRS SV was then placed where the lowest ADC values were found, compatibly with the lesion site and size.

^{1}H-magnetic resonance spectroscopy

Single-voxel (SV) MRS point-resolved spectroscopy (PRESS) sequences with TE = 30 ms (TE1/TE2/TR = 20/10/2000 ms; 144 averages) and TE = 97 ms (TE1/TE2/TR = 32/65/2000 ms; 160 averages) were performed, tailored using numerical simulation in order to maximize the 2HG 2.25-ppm signal detection, leading to improved differentiation between 2HG and nearby GABA, glutamine (Gln), and Glu signals. These sequences were previously implemented by another group [9, 10], and we more recently optimized the TE30 sequence on our scanner in a phantom study [8].

1.5 × 1.5 × 1.5-cm^3 and 2 × 2 × 2-cm^3 voxel sizes were tested.

Two identical SVs were acquired: one in the lesion and one in the contralateral hemisphere.

Each MRS sequence took about 6-min time scan.

Table 1 Previous in vivo 2HG-MRS studies on human glioma patients

Study	No. of subjects	MRS technique	MR scanner	Study aim (diagnosis, FU)
Choi et al. [10]	30 gliomas (15 IDHmut[4], 15 wt[5])	PRESS, TE 97 ms and 106 ms, SV, voxel 2^3 cm^3, and MV (1 pt)	3 T	Diagnosis
Pope et al. [11]	24 gliomas (9 IDHmut, 15 wt)	PRESS, TE 30 ms, SV, voxel 2^3 cm^3	3 T	Diagnosis
Andronesi et al. [12]	6 gliomas (2 IDHmut, 4 wt), 4 healthy controls	2D LASER-COSY, 1D MEGALASER, 1D LASER, voxel 3^3 cm^3	3 T	Diagnosis
Choi et al. [9]	22 IDHmut gliomas, 7 healthy controls	PRESS, TE 35 ms and 97 ms, SV, voxel 2^3 cm^3	3 T	Diagnosis
Natsumeda et al. [5]	52 gliomas (25 IDHmut, 27 wt)	PRESS, TE 30 ms, SV, voxel $12–20^3$ mm^3	3 T	Diagnosis, FU
Emir et al. [13]	14 gliomas (10 IDHmut, 4 wt), 8 healthy controls	Semi-LASER, SV, voxel 2^3 cm^3	7 T	Diagnosis
Andronesi et al. [14]	25 IDHmut gliomas	MEGALASER, voxel 2^3 cm^3	3 T	Diagnosis, FU (13 pts)
De la Fuente et al. [15]	89 gliomas (80 IDHmut, 9 wt)	PRESS, TE 97 ms, SV, variable voxel size	3 T	Diagnosis, FU (1 pt)
Nagashima et al. [16]	47 gliomas (18 IDHmut, 29 wt)	PRESS, TE 35 ms, SV, voxel 1.5^3 cm^3	3 T	Diagnosis
Bisdas et al. [17]	16 gliomas (11 IDHmut, 5 wt)	STEAM, TE 20 ms, MV, voxel 1^3 cm^3	9.4 T	Diagnosis
Ganji et al. [18]	12 gliomas (6 IDHmut, 6 IDH unknown)	PRESS, TE 78 ms, STEAM, TE 13 ms, SV, voxel 2^3 cm^3	7 T	Diagnosis
An et al. [19]	15 IDHmut gliomas	Triple-refocus, TE 137 ms, SV, variable voxel size	3 T	Diagnosis
Jafari-Khouzani et al. [20]	17 IDHmut gliomas		3 T	FU
Andronesi et al. [21]	25 IDHmut gliomas	MEGALASER, MV	3 T	FU (RT-CHT)
Choi et al. [22]	136 gliomas	PRESS MV	3 T	Diagnosis, FU
Berrington et al. [23]	11 gliomas	SEMILASER, PRESS TE 97 ms voxel 2^3 cm^3	3 T	Diagnosis
Crisi et al. [24]	82 gliomas (26 IDHmut[4], 56 wt[5])	PRESS TE 35 ms, SV	3 T	Diagnosis
Tietze et al. [25]	30 gliomas	PRESS	3 T	Diagnosis
Branzoli et al. [26]	24 gliomas	MEGAPRESS, PRESS TE 97 ms	3 T	Diagnosis
An et al. [27]	4 gliomas (3 IDHmut, 1 wt)	EPSI	7 T	Diagnosis
Zhou et al. [28]	85 gliomas	PRESS TE 97 ms	3 T	Diagnosis, FU
Andronesi et al. [29]	8 IDH1mut gliomas	MEGALASER, MV	3 T	IDH305-treated patients FU[4]

MRS, magnetic resonance spectroscopy; *MR*, m*agnetic* resonance (T = Tesla); *FU*, follow-up; *IDHmut*, IDH mutated; wt, IDH wild type; *PRESS*, point-resolved spectroscopy; *SV*, single voxel; *MV*, multivoxel; *COSY*, COrrelation S*pectroscopy*; *STEAM*, stimulated echo acquisition mode; *RT-CHT*, radiotherapy-chemotherapy; *EPSI*, echo-planar spectroscopic imaging, *IDH305*, IDH1 inhibitor

LCModel

All spectra were analyzed using LCModel software version 6.3 [30] performing phase correction and using a linear combination of spectra from a simulated metabolite basis-set including 20 metabolites [10]. A spectrum with the same sequence parameters but no water-suppression was acquired before every PRESS sequence and employed as reference for the evaluation of absolute concentration. Concentration uncertainties were estimated using Cramér-Rao lower bounds (CRLBs), and 20% was considered as reliability limit [30].

See Online Resource (Supplementary Methods) for Histopathology, DNA sequencing of *IDH1/2* genes, loss of heterozygosity (LOH) analysis, O^6-methylguanine-DNA-methyltransferase (MGMT) promoter hypermethylation analysis by PCR on tissue samples, and circulating 2HG analysis.

Statistical analysis

Descriptive statistics were used to describe all variables recorded in this study. Significant associations were assessed with the use of Mann-Whitney test and Chi-square or Fisher exact test. Continuous variables were further analyzed through receiver operating characteristic (ROC) curves in order to identify the best cutoff in terms of sensitivity and specificity to distinguish patients in relation to *IDH*, 1p19q LOH, and

MGMT promoter methylation status. As proposed by others [29], the optimal cutoff values were chosen to optimize specificity with sensitivity above 50%.

A logistic regression analysis was performed to assess whether measured metabolites could be used to discriminate between two patient groups based on *IDH*, 1p/19q LOH, and *MGMT* promoter methylation. First, for each metabolite (i.e., predictor), univariate logistic models were performed. Second, if 2HG and metabolites were detected at significant levels by univariate test, 2HG associated to another metabolite were entered as predictors in a single block multivariate logistic regression to assess if the prediction of this model improved in comparison with univariate logistic regression. Goodness of fit of the model was evaluated with Hosmer statistics for small samples.

Results

Fifty-nine patients were studied by MRS, underwent subsequent surgery, obtained histological diagnosis, and were investigated for the *IDH* mutation by histology or Sanger sequencing. Median time between MRS and neurosurgery was 6 days (range 1–37 days). Three cohorts of patients were studied with different MRS protocols.

The first cohort included 13 subjects (10 *IDH*mut, 3 *IDH*wt) and underwent MRS by the TE30 ms: only in 5 cases, 2HG peak corresponded to the *IDH* status; four cases were false negative (FN); two were false positive (FP) within tumor voxels; and FP also resulted in contralateral voxels.

The second cohort was studied by the TE 97 ms sequence with voxel 1.5 × 1.5 × 1.5 cm^3 and included 14 subjects (10 *IDH*mut, 4 *IDH*wt). No contralateral FP were found, but there were six FN and two FP in tumor voxels.

Given the low accuracy, the above sequences were abandoned and a third cohort was studied.

A TE 97 ms sequence with larger voxel (2 × 2 × 2 cm^3) was used in the last 32 patients, including 19 *IDH*mut and 13 *IDH*wt. 2HG could be quantified in 15/19 *IDH*mut gliomas (Fig. 1a) with CRLB ≤ 20% in all of true positive (TP) cases. True negative (TN) spectra (11/13 *IDH*wt) showed absence of detectable 2HG (concentration 0, CRLB 999%) (Fig. 1b). 2HG was never detected in contralateral voxels.

Two cases with 1.85 and 1.3 mM 2HG at MRS analysis showed CRLB above the 20% limit (respectively 36% and 47%), suggesting low reliability, and were thus erased from subsequent analyses. Both were *IDH1*wt on IHC; *IDH1/2* PCR analysis resulted negative for one patient, while for the other one tumoral tissue was insufficient to perform PCR (Fig. 1c).

The four FN included one case in which tumor volume (3.2 cm^3) was smaller than the voxel size (Fig. 1d), and three with relative ADC (rADC) 1.6–1.9, suggesting low cellularity according to tumoral cell density evaluation (scale: cell number < 20, low (L); cell number 20–25, medium (M); cell number ≥ 26, high (H)) on histological specimens (see Supplementary Methods), as displayed in Table 2.

Statistical analysis focused on the third cohort. Patient characteristics, histological diagnosis, molecular assessment, and 2HG level by brain MRS are shown in Table 2.

The presence of 2HG on MRS was associated with *IDH* mutations ($P = 0.001$, Fisher's exact test). MRS showed 79% (95% confidence interval (CI), 54.43–93.95%) sensitivity, 100% (95% CI, 71.51–100%) specificity, and 87% (95% CI, 69.28–96.24 %) accuracy with respect to the IDH status. Area under the curves (AUC) was 0.895 (95% CI: 0.756–1).

1p19q codeleted gliomas (oligodendrogliomas: ODG) exhibited more frequently IDH mutations ($P = 0.009$, chi-square test) than 1p19q non-codel gliomas (astrocytomas: A) and 2HG-MRS levels were higher (Mann-Whitney test) (Table 3). Using ROC analysis, 2HG cutoff of 0.75 differentiated the two types with sensitivity of 66.7% and specificity of 81.3%. AUC was 0.77 (95% CI, 0.574–0.967).

Only one out of four GBM was *IDH*mut.

A 2HG cutoff 0.65 showed 60% sensitivity and 91.7% specificity to differentiate *MGMT* promoter methylation status; the AUC was 0.72 (95% CI, 0.526–0.919).

10q loss was more frequent in *IDH*wt ($P = 0.03$, Fisher's exact test).

Aside from 2HG, lower concentrations of creatine (Cr), Glu, myo-inositol (mI), and glutathione (GSH) were found in *IDH*mut than in *IDH*wt gliomas (Mann-Whitney test) (Table 3). AUC were 0.73 (95% CI, 0.542–0.911), 0.86 (95% CI, 0.695–1), 0.85 (95% CI, 0.715–0.989), and 0.73 (95% CI, 0.557–0.912), respectively. Using ROC analysis, we investigated the metabolites' levels in determining *IDH*-mutation status in the cohort. Cutoff values were 2.1 for Cr (sensitivity of 54% and specificity of 89.5%), 2.65 for Glu (sensitivity of 77% and specificity of 95%), 4.7 for mI (sensitivity of 77% and specificity of 84%), and 0.35 for GSH (sensitivity of 61.5% and specificity of 68.5%) respectively.

In the patient classification for *IDH*, univariate logistic regressions were significant for 2HG, Glu, mI, and GSH (Table 4). Forward and backward logistic regression including cross-validation showed that the goodness of fit of the model in multivariate logistic regression gained 93.5% prediction to diagnose IDH mutation combining 2HG, Glu, and mI ($P <$ 0.01, omnibus chi-square, Hosmer and Lameshow).

ROC curves for MRS metabolites and IDH, 1p19q, and MGMT status are shown in Supplementary Data (Figure 1S).

Serum samples from 22 patients and urine samples from 13 patients of cohort 3 were analyzed to measure 2HG: no significant differences were found in *IDH*mut vs *IDH*wt.

Patients carrying *IDH* mutations were younger than wt (median 34 vs 55 yrs, $P = 0.005$), as expected (Mann-Whitney test). *IDH* status did not significantly correlate to

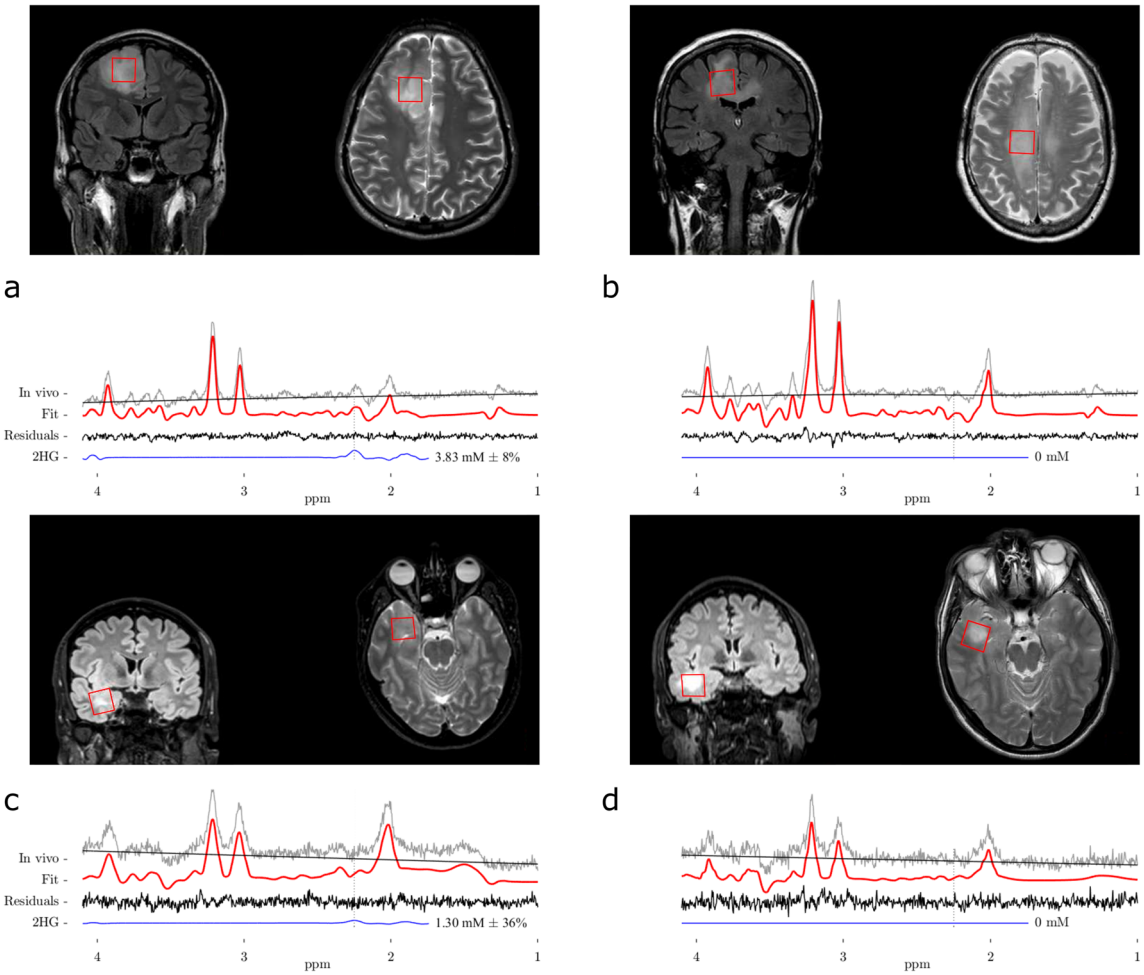

Fig. 1 Panel showing some representative cases. **a** True positive (TP), patient 20. **b** True negative (TN), patient 30. **c** Unreliable MRS result: small tumor (volume 1.6 cm^3) showing 1.85 mM 2HG level but CRLB exhibiting low reliability (36%). IHC was negative for IDH1 R132H mutation, while tumoral tissue was not enough to perform PCR analysis. **d** False negative (FN), patient 8: small tumor (volume 3.4 cm^3) with low cellularity and proliferation index

gender, lesion site, contrast enhancement, tumor grade, concentrations of metabolites other than those above described (Table 2), p53, ATRX, TERT, and MIB-1 (proliferation index).

Discussion

Diagnosis and classification of gliomas are based on tissue histology integrated with molecular markers [1, 4]. In LGG, these markers include *IDH1/2* status, 1p/19q codeletion, 10q deletion, TERT and ATRX mutation, and *MGMT* promoter methylation status [4]. *IDH* mutations have prognostic relevance irrespective of glioma grade [4].

In vivo brain metabolite imaging provides a unique opportunity for the evaluation of the lesion and surrounding tissue: specifically, 2HG-MRS may help define the infiltrative tumor area, guiding surgical and radiotherapeutic approaches, and can be useful to monitor treatment response to cytoreductive or IDH-targeted therapies [2, 15, 20–22, 29, 31–35].

We enrolled adult patients with suspected LGG scheduled for surgery, aiming to evaluate the clinical feasibility and accuracy of 2HG-MRS. *IDH*mut and wt gliomas were represented, and we analyzed histological type and grade, the salient molecular features, radiological features as tumor site, contrast enhancement and ADC, and the main MRS metabolites, in order to find correlations with *IDH* status. Various techniques have been proposed to perform 2HG-MRS: PRESS, MEGAPRESS, and MEGALASER have been found to exhibit good accuracy, with some limitations in specific setting series [6]. Some authors reported better accuracy of MEGAPRESS with respect to PRESS [12, 26], differently from Choi et al. [10]. We decided to use PRESS to enhance the 2.25-ppm 2HG peak, which is most represented at 3 T. Two TE (30 and 97 ms) and voxel sizes were assessed: after confirmation by phantom study that TE 97 is more accurate than TE 30 (data not showed), we focalized on TE 97 in study

Table 2 Demographic features and main characteristics of the patients, including histology, proliferation index (MIB-1), cell density, *IDH* status, and main molecular data

Pt	Gender	Age	Site	T1mdc CE	Histology	Grade	MIB-1 (%)	Cell density	IDHmut (IHC/PCR)	LOH 1p	LOH 19q	LOH 10q	MGMT	p53	ATRX	TERT	MRS 2HG
1	F	61	f-p	Yes	A A	III	6–7	M	Neg/NA	NA	NA	NA	NA	Neg	NA	NA	Undetectable
2	M	28	f	No	A	II	2–	L	R132H	Yes	No	No	Unmet	Pos	Neg	Pos	0.2
3	M	15	f	No	ODG	II	2	H	R132H	Yes	Yes	No	Unmet	Neg	Pos	Pos	0.4
4	M	38	f	No	A	II	3–4	L	R132H	No	No	Yes	Unmet	Pos	Neg	Pos	Undetectable
5	F	59	f-t-p	No	A ODG	III	6–7	M	R132H	Yes	Yes	No	Met	Neg	Pos	Pos	0.9
6	F	46	t-p	No	A ODG	III	5–6	M	R132H	Yes	Yes	Yes	Met	Pos	Neg	Neg	0.8
7	M	66	t	No	A A	III	7–8	L	Neg	No	No	Yes	Unmet	Neg	Pos	Pos	Undetectable
8	M	35	t	No	ODG	II	2–3	L	R132H	Yes	Yes	No	Met	Neg	Pos	Pos	Undetectable
9	M	43	t-i	No	ODG	II	1–2	L	R132H	Yes	Yes	No	Unmet		Neg	Neg	1.6
10	M	31	f	Yes	A A	III	7–8	H	R132H	Yes	No	No	Met	Pos	Neg	Neg	0.7
11	F	34	t	Yes	ODG	II	7–8	H	R132H	No	No	No	Unmet	Neg	Pos	Pos	0.3
12	M	65	f-t-p	Yes	GBM	IV	12–15	M	Neg				Met	Pos	NA	NA	Undetectable
13	F	28	p	Yes	ODG	II	5–6	M	R132H	Yes	Yes	No	Met	Neg	Pos	Neg	0.4
14	M	62	t	Yes	GBM	IV	20	H	Neg				Met	Neg	Pos	Neg	Undetectable
15	M	54	i	No	A A	III	7–8	L	R132H	No	Yes	Yes	Unmet	Neg	Neg	Neg	0.6
16	M	55	f - i	Yes	GBM	IV	30	H	Neg				Met	Neg	Pos	Pos	Undetectable
17	M	41	f-t-i	No	A A	III	1	L	R132H	No	No	No	Met	Pos	Neg	Neg	1.4
18	F	23	f	No	A A	III	6–7	L	R132H	No	No	No	Unmet	Pos	Pos	Neg	Undetectable
19	M	46	f	Yes	GBM	IV	15–20	M	R132G				Met	Pos	Pos	Pos	Undetectable
20	M	23	f	Yes	A ODG	III	70	H	R132H	Loss	No	No	Met	Neg	Pos	Neg	3.8
21	M	32	Thalamus	No	AF	II	5–6	L	Neg	No	No	No	Unmet	Neg	Neg	Neg	Undetectable
22	F	44	f	No	A	II	4–5	L	R132H	No	Yes	No	Unmet	Neg	ND	Neg	Undetectable
23	M	15	t	No	GBM	IV	25–30	H	Neg				Unmet	Pos	Pos	Neg	Undetectable
24	M	32	f-t-i	No	ODG	II	2–3	M	R132H	Yes	Yes	No	Met	Neg	Pos	Pos	4.6
25	M	52	t-i	No	A ODG	III	4–6	M	R132H	Yes	Yes	No	Met	Pos	NE	Pos	1.7
26	F	48	t-i	No	A	II	5–6	L	Neg	Yes	No	Yes	Unmet		Pos	Neg	Undetectable
27	M	23	t	No	ODG	II	1–2	L	R132H	Yes	Yes	No	Met	Neg	Pos	Neg	2.5
28	M	60	f	Yes	A A	III	7–8	M	Neg	No	Yes	Yes	Unmet	Neg	Pos	Neg	Undetectable
29	M	30	f-t-i	No	A	II	2–3	L	R132H	No	No	No	Met	Pos	Neg	Pos	0.7
30	F	76	CC-f bilat	No	A	II	3	L	Neg	No	No	No	Met	Neg	Pos	Pos	Undetectable

f, frontal; *p*, parietal; *t*, temporal; *i*, insular; *cc*, corpus callosum;*T1mdc CE*, T1-sequence MRI with contrast enhancement; *ODG*, oligodendroglioma; *A ODG*, anaplastic ODG; *A*, astrocytoma; *A A*, anaplastic A; *NA*, not available tissue

Table 3 Median metabolite levels and IDH, 1p19q, MGMT status. *P* values of significant differences are also shown

	IDHwt	IDHmut	*P*	1p19q hetero	1p19q LOH	*P*	MGMT met	MGMT unmet	*P*
2HG	Undetectable	1.1	***	0.8	2	*	0.4	0.2	*
Cr	2.2	1.2	*						
Glu	3.4	1.5	***						
mI	5.5	3.6	***						
GSH	0.4	0.2	*						

*$P < 0.05$

**$P < 0.005$

***$P < 0.001$

patients. The first cohort was assessed using smaller voxel size, and later, based also on the literature, we moved forward and evaluated larger voxel. Likewise with Choi et al. [9], we confirmed in our cohort that TE 97 ms with the larger voxel (2 × 2 × 2 cm^3) shows high accuracy. By this procedure, 2HG-MRS showed 79% sensitivity and 100% specificity with respect to the IDH status.

A contribution of our study is that we studied a prospective, homogeneous cohort of treatment-naïve consecutive patients with suspect lower-grade gliomas and we showed the gain of a good diagnostic accuracy of 2HG-MRS with TP spectra showing CRLB below 20%, a reliability limit used also in other studies [9, 12]. We excluded only two patients whose spectra showed CRLB > 20%, thus unreliable.

We addressed the issue using a technology (3 T scanner, LCModel software) available for clinical practice and MRS sequences lasting around 6 min.

Moreover, we expanded the evaluation to MRS analysis to other brain metabolites and molecular features. In particular, we found that the combination of Glu and mI with 2HG improved diagnostic accuracy. The decrease in Glu concentrations observed in our sample is consistent with the documented production of 2HG from Glu-derived α-KG through Glu [16, 36]. mI is an osmolyte normally present in astrocytes, involved in cell membrane and myelin sheet. Our results of significantly higher levels of mI in IDH1 wt glioma may support its role as promoter of PKC activation associated with the aggressive behavior of high-grade gliomas [37].

Our study found difference in 2HG level between ODG and A, as recently reported [36] using ex vivo proton high-resolution magic angle spinning spectroscopy on glioma tissue samples. The relationship between 2HG and *MGMT* methylation is coherent with the tight association between MGMT methylation and IDH mutation in gliomas [38].

Table 4 Univariate logistic regressions for significant metabolites in the patient classification for IDH

Metabolite	Goodness of fit (%)	ODD ratio	*P* value (Wald test)
2HG	86.7	1091	0.000
Glu	86.7	0.24	0.007
mI	73.3	0.67	0.044
GSH	66.7	0.01	0.039

Present study carries some limitations. MRS levels of 2HG in the majority of our patients were quite low, in spite of the good reliability (detected by CRLB). Although a recent meta-analysis identified 1.76 mM as cutoff to determine the presence of 2HG on MRS [6], in our study we found that lower levels of 2HG with CRLB < 20% identified *IDH* mutant gliomas while in *IDH* wild-type 2HG was undetectable (concentration 0, CRLB 999%) in TN cases.

FN spectroscopic results were found in one small glioma and in three lesions with low cellularity, in agreement with previous data [9]. Two cases were excluded because 2HG was measured by MRS but CRLB was above the reliability limit; both were IDHwt at IHC: one of these tumors was very small and PCR could not be performed, and the other patient was a 38-year-old man carrying a not-enhancing *IDH*wt anaplastic A, with tumor volume smaller than voxel size.

In a cohort of patients, we tried to quantify 2HG in plasma and urine samples, as previously performed with inconclusive results [7, 39, 40]: we assessed pre-surgery 2HG level in plasma and urine by LC-MS, without finding a significant association between circulating 2HG and *IDH* status. Our 2HG level range is aligned with that reported by Fathi et al. for glioma patients.

Although intratumoral 2HG accumulation provides a marker for the presence of *IDH* mutations, circulating 2HG may not yet be a useful marker for glioma molecular classification: further approaches need to get an actionable-reproducible test.

In summary, our data confirm that non-invasive detection and quantification of 2HG by MRS are clinically feasible at 3 T using PRESS TE 97 ms with good diagnostic performance [6].

Association with other metabolites evaluable by MRS may increase the diagnostic and predictive value of 2HG testing.

Further investigations in multi-institutional studies are needed to achieve unambiguous and reproducible accuracy

widely applicable in clinical settings of SV and MV 2HG-MRS to improve LGG diagnosis and to facilitate personalized treatments (NCT02193347; NCT03343197, NCT02454634, NCT02481154, NCT02273739,. NCT02381886) and follow-up [15, 20, 21, 29; NCT03952598, NCT03677999].

Acknowledgements We thank Federico Riccardi Sirtori (Oncology Unit, Nerviano Medical Sciences, Nerviano (MI)) for dosing 2HG in biological fluids and Ruben Gianeri (Unit of Neuroradiology, FONDAZIONE IRCCS ISTITUTO NEUROLOGICO CARLO BESTA) for the help with MR imaging. We absolutely thank our patients.

Compliance with ethical standards

The Institutional Ethics Committee approved the study (protocol n. 419/2014), which conforms to the Declaration of Helsinki. Informed consent was obtained from all participants.

Conflict of interest The authors declare that they have no conflict of interest.

References

1. Louis DN, Perry A, Reifenberger G, von Deimling A, Figarella-Branger D, Cavenee WK, Ohgaki H, Wiestler OD, Kleihues P, Ellison DW (2016) The 2016 World Health Organization classification of tumors of the central nervous system: a summary. Acta Neuropathol 131(6):803–820
2. Dang L, Yen K, Atta EC (2016) IDH mutations in cancer and progress toward development of targeted therapeutics. Ann Oncol 27:599–608
3. Yan H, Parsons DW, Jin G, McLendon R, Rasheed BA, Yuan W, Kos I, Batinic-Haberle I, Jones S, Riggins GJ, Friedman H, Friedman A, Reardon D, Herndon J, Kinzler KW, Velculescu VE, Vogelstein B, Bigner DD (2009) IDH1 and IDH2 mutations in gliomas. N Engl J Med 360:765–773
4. Brat DJ, Verhaak RG, Aldape KD et al (2015) Comprehensive, integrative genomic analysis of diffuse lower-grade gliomas. N Engl J Med 372(26):2481–2498
5. Natsumeda M, Igarashi H, Nomura T et al (2014) Accumulation of 2-hydroxyglutarate in gliomas correlates with survival: a study by 3.0-tesla magnetic resonance spectroscopy. Acta Neuropathologica. Communications 2:158
6. Suh CH, Kim HS, Jung SC, Choi CG, Kim SJ (2018) 2-hydroxyglutarate MR Spectroscopy for prediction of isocitrate dehydrogenase mutant glioma: a systemic review and meta-analysis using individual patient data. Neuro-Oncology 20(12):1573–1583. https://doi.org/10.1093/neuonc/noy113
7. Lombardi G, Corona G, Bellu L, Della Puppa A, Pambuku A, Fiduccia P, Bertorelle R, Gardiman MP, D'Avella D, Toffoli G, Zagonel V (2015) Diagnostic value of plasma and urinary 2-hydroxyglutarate to identify patients with isocitrate dehydrogenase-mutated glioma. Oncologist 20(5):562–567
8. Bertolino N, Marchionni C, Ghielmetti F, Burns B, Finocchiaro G, Anghileri E, Bruzzone MG, Minati L (2014) Accuracy of 2-hydroxyglutarate quantification by short-echo proton-MRS at 3T: a phantom study. Phys Med 30(6):702–707
9. Choi C, Ganji S, Hulsey K, Madan A, Kovacs Z, Dimitrov I, Zhang S, Pichumani K, Mendelsohn D, Mickey B, Malloy C, Bachoo R, Deberardinis R, Maher E (2013) A comparative study of short- and long-TE ^{1}H-MRS at 3T for in-vivo detection of 2-hydroxyglutarate in brain tumors. NMR Biomed 26(10):1242–1250
10. Choi C, Ganji SK, DeBerardinis RJ et al (2012) 2-hydroxyglutarate detection by magnetic resonance spectroscopy in IDH-mutated glioma patients. Nat Med 18(4):624–629
11. Pope WB, Prins RM, Albert Thomas M, Nagarajan R, Yen KE, Bittinger MA, Salamon N, Chou AP, Yong WH, Soto H, Wilson N, Driggers E, Jang HG, Su SM, Schenkein DP, Lai A, Cloughesy TF, Kornblum HI, Wu H, Fantin VR, Liau LM (2012) Non-invasive detection of 2-hydroxyglutarate and other metabolites in IDH1 mutant glioma patients using magnetic resonance spectroscopy. J Neuro-Oncol 107(1):197–205
12. Andronesi OC, Kim GS, Gerstner E et al (2012) Detection of 2-Hydroxyglutarate in IDH-mutated Glioma Patients by Spectral-editing and 2D Correlation Magnetic Resonance Spectroscopy. Sci Transl Med 4(116):116ra4
13. Emir UE, Larkin SJ, de Pennington N, Voets N, Plaha P, Stacey R, al-Qahtani K, Mccullagh J, Schofield CJ, Clare S, Jezzard P, Cadoux-Hudson T, Ansorge O (2016) Noninvasive quantification of 2-hydroxyglutarate in human gliomas with IDH1 and IDH2 mutations. Cancer Res 76(1):43–49
14. Andronesi OC, Rapalino O, Gerstner E et al (2013) Detection of oncogenic IDH1 mutations using magnetic resonance spectroscopy of 2-hydroxyglutarate. J Clin Invest 123(9):3659–3663
15. De la Fuente MI, Young RJ, Rubel J et al (2016) Integration of 2-hydroxyglutarate-proton magnetic resonance spectroscopy into clinical practice for disease monitoring in isocitrate dehydrogenase-mutant glioma. Neuro-Oncology 18(2):283–290
16. Nagashima H, Tanaka K, Sasayama T, Irino Y, Sato N, Takeuchi Y, Kyotani K, Mukasa A, Mizukawa K, Sakata J, Yamamoto Y, Hosoda K, Itoh T, Sasaki R, Kohmura E (2016) Diagnostic value of glutamate with 2-hydroxyglutarate in magnetic resonance spectroscopy for IDH1 mutant glioma. Neuro-Oncology 18(11):1559–1568
17. Bisdas S, Chadzynski GL, Braun C, Schittenhelm J, Skardelly M, Hagberg GE, Ethofer T, Pohmann R, Shajan G, Engelmann J, Tabatabai G, Ziemann U, Ernemann U, Scheffler K (2016) MR spectroscopy for in vivo assessment of the oncometabolite 2-hydroxyglutarate and its effects on cellular metabolism in human brain gliomas at 9.4T. J Magn Reson Imaging 44(4):823–833
18. Ganji SK, An Z, Tiwari V, McNeil S, Pinho MC, Pan E, Mickey BE, Maher EA, Choi C (2017) In vivo detection of 2-hydroxyglutarate in brain tumors by optimized point-resolved spectroscopy (PRESS) at 7T. Magn Reson Med 77(3):936–944
19. An Z, Ganji SK, Tiwari V, Pinho MC, Patel T, Barnett S, Pan E, Mickey BE, Maher EA, Choi C (2017) Detection of 2-hydroxyglutarate in brain tumors by triple-refocusing MR spectroscopy at 3T in vivo. Magn Reson Med 78(1):40–48
20. Jafari-Khouzani K, Loebel F, Bogner W, Rapalino O, Gonzalez GR, Gerstner E, Chi AS, Batchelor TT, Rosen BR, Unkelbach J, Shih HA, Cahill DP, Andronesi OC (2016) Volumetric relationship between 2-hydroxyglutarate and FLAIR hyperintensity has potential implications for radiotherapy planning of mutant IDH glioma patients. Neuro-Oncology 18(11):1569–1578
21. Andronesi OC, Loebel F, Bogner W, Marjańska M, Vander Heiden MG, Iafrate AJ, Dietrich J, Batchelor TT, Gerstner ER, Kaelin WG, Chi AS, Rosen BR, Cahill DP (2016) Treatment response assessment in IDH-mutant glioma patients by non-invasive 3D functional spectroscopic mapping of 2-hydroxyglutarate. Clin Cancer Res 22(7):1632–1641
22. Choi C, Raisanen JM, Ganji SK, Zhang S, McNeil S, An Z, Madan A, Hatanpaa KJ, Vemireddy V, Sheppard CA, Oliver D, Hulsey KM, Tiwari V, Mashimo T, Battiste J, Barnett S, Madden CJ, Patel TR, Pan E, Malloy CR, Mickey BE, Bachoo RM, Maher EA (2016) Prospective longitudinal analysis of 2-hydroxyglutarate magnetic resonance spectroscopy identifies broad

clinical utility for the management of patients with IDH-mutant glioma. J Clin Oncol 34(33):4030–4039
23. Berrington A, Voets NL, Plaha P, Larkin SJ, Mccullagh J, Stacey R, Yildirim M, Schofield CJ, Jezzard P, Cadoux-Hudson T, Ansorge O, Emir UE (2016) Improved localisation for 2-hydroxyglutarate detection at 3T using long-TE semi-LASER. Tomography 2(2):94–105
24. Crisi G, Filice S, Michiara M, Crafa P, Lana S (2018) 2-Hydroxyglutarate detection by short echo time magnetic resonance spectroscopy in routine imaging study of brain glioma at 3.0 T. J Comput Assist Tomogr 42(3):469–474
25. Tietze A, Choi C, Mickey B, Maher EA, Parm Ulhøi B, Sangill R, Lassen-Ramshad Y, Lukacova S, Østergaard L, von Oettingen G (2018) Noninvasive assessment of isocitrate dehydrogenase mutation status in cerebral gliomas by magnetic resonance spectroscopy in a clinical setting. J Neurosurg 128(2):391–398
26. Branzoli F, Di Stefano AL, Capelle L et al (2018) Highly specific determination of IDH status using edited in vivo magnetic resonance spectroscopy. Neuro-Oncology 20(7):907–916
27. An Z, Tiwari V, Ganji SK (2018) Echo-planar spectroscopic imaging with dual-readout alternated gradients (DRAG-EPSI) at 7 T: application for 2-hydroxyglutarate imaging in glioma patients. Magn Reson Med 79(4):1851–1861
28. Zhou M, Zhou Y, Liao H, Rowland BC, Kong X, Arvold ND, Reardon DA, Wen PY, Lin AP, Huang RY (2018) Diagnostic accuracy of 2-hydroxyglutarate magnetic resonance spectroscopy in newly-diagnosed brain mass and suspected recurrent gliomas. Neuro-Oncology 20(9):1262–1271
29. Andronesi OC, Arrillaga-Romany IC, Ly KI et al (2018) Pharmacodynamics of mutant-IDH1 inhibitors in glioma patients probed by in vivo 3D MRS imaging of 2-hydroxyglutarate. Nat Commun 9(1):1474
30. Provencher SW (2001) Automatic quantitation of localized in vivo 1H spectra with LCModel. NMR Biomed 14(4):260–264
31. Pellegatta S, Valletta L, Corbetta C et al (2015) Effective immune-targeting of the IDH1 mutation R132H in a murine model of intracranial glioma. Acta Neuropathol Commun 3:4
32. Schumacher T, Bunse L, Wick W, Platten M (2015) Mutant IDH1: an immunotherapeutic target in tumors. Oncoimmunology 3(12): e974392
33. Pusch S, Krausert S, Fischer V, Balss J, Ott M, Schrimpf D, Capper D, Sahm F, Eisel J, Beck AC, Jugold M, Eichwald V, Kaulfuss S, Panknin O, Rehwinkel H, Zimmermann K, Hillig RC, Guenther J, Toschi L, Neuhaus R, Haegebart A, Hess-Stumpp H, Bauser M, Wick W, Unterberg A, Herold-Mende C, Platten M, von Deimling A (2017) Pan-mutant IDH1 inhibitor BAY 1436032 for effective treatment of IDH1 mutant astrocytoma in vivo. Acta Neuropathol 133(4):629–644
34. Wijnenga MMJ, French PJ, Dubbink HJ, Dinjens WNM, Atmodimedjo PN, Kros JM, Smits M, Gahrmann R, Rutten GJ, Verheul JB, Fleischeuer R, Dirven CMF, Vincent AJPE, van den Bent M (2018) The impact of surgery in molecularly defined low-grade glioma: an integrated clinical, radiological, and molecular analysis. Neuro-Oncology 20(1):103–112
35. Waitkus MS, Diplas BH, Yan H (2018) Biological role and therapeutic potential of IDH mutations in cancer. Cancer Cell 34(2):186–195
36. Jalbert LE, Elkhaled A, Phillips JJ et al (2017) Metabolic profiling of IDH mutation and malignant progression in infiltrating glioma. Sci Rep 7:44792
37. do Carmo A, Balça-Silva J, Matias D, Lopes MC (2013) PKC signaling in glioblastoma. Cancer Biol Ther 14(4):287–294
38. Turcan S, Rohle D, Goenka A, Walsh LA, Fang F, Yilmaz E, Campos C, Fabius AW, Lu C, Ward PS, Thompson CB, Kaufman A, Guryanova O, Levine R, Heguy A, Viale A, Morris LG, Huse JT, Mellinghoff IK, Chan TA (2012) IDH1 mutation is sufficient to establish the glioma hypermethylator phenotype. Nature 483(7390):479–483
39. Fathi AT, Nahed BV, Wander SA, Iafrate AJ, Borger DR, Hu R, Thabet A, Cahill DP, Perry AM, Joseph CP, Muzikansky A, Chi AS (2016) Elevation of urinary 2-hydroxyglutarate in IDH-mutant glioma. Oncologist 21(2):214–219
40. Capper D, Simon M, Langhans CD, Okun JG, Tonn JC, Weller M, von Deimling A, Hartmann C, German Glioma Network (2012) 2-Hydroxyglutarate concentration in serum from patients with gliomas does not correlate with IDH1/2 mutation status or tumor size. Int J Cancer 131:766–768